

# Formation of Carboxylic Acids from Alcohols and Olefins in Zeolite H-ZSM-5 under Mild Conditions via Trapping of Alkyl Carbenium Ions with Carbon Monoxide: An *in Situ* $^{13}\text{C}$ Solid State NMR Study

Alexander G. Stepanov,\* Mikhail V. Luzgin, Vyacheslav N. Romannikov, Vladimir N. Sidelnikov, and Kirill I. Zamaraev†

*Boreshkov Institute of Catalysis, Siberian Branch of the Russian Academy of Sciences, Prospekt Akademika Lavrentieva 5, Novosibirsk 630090, Russia*

Received April 10, 1996; revised August 16, 1996; accepted August 19, 1996

Using *in situ*  $^{13}\text{C}$  solid state MAS NMR (for some reagents in combination with *ex situ* GC-MS), it is shown that butyl alcohols and olefins (ethene, isobutene, octene-1) undergo carbonylation to form carboxylic acids (the Koch reaction) with high conversion on zeolite H-ZSM-5 at 296–373 K. The reactions proceed without application of pressurized conditions, just upon coadsorption of CO and alcohols or CO,  $\text{H}_2\text{O}$ , and olefins on zeolite. The observed Koch reaction under mild conditions provides strong evidence for the formation of alkyl carbenium ions from alcohols and olefins on the zeolites as crucial reaction intermediates. Of the family of carbenium ions, CO reacts selectively with tertiary cations to produce tertiary carboxylic acids, unless the carbonylated molecule is too large for more bulky tertiary moieties to be accommodated and carbonylated in the narrow pores of H-ZSM-5. Thus, *t*-BuOH, *i*-BuOH, and isobutene produce trimethylacetic acid with high selectivity and conversion, while ethene transforms selectively into 2-methyl-2-ethyl butyric acid. Reaction of octene-1 molecules with CO and  $\text{H}_2\text{O}$  results in acids of the  $\text{C}_8\text{H}_{17}\text{COOH}$  and  $\text{C}_{16}\text{H}_{33}\text{COOH}$  families with predominantly linear hydrocarbon chains. The data obtained may open up new possibilities in using solid acids in organic synthesis as carbonylation catalysts under mild conditions, i.e., low temperature and normal atmospheric pressure. © 1996 Academic Press, Inc.

## 1. INTRODUCTION

By analogy with reactions in acid solutions, it is generally agreed that hydrocarbon conversion on solid acids proceeds via the formation of intermediate carbenium ions (1, 2). Contrary to superacid solutions where carbenium ions were indeed detected and well characterized (3–5), actual evidences for the existence of carbenium ion intermediates on solid acids are not that straightforward. Their existence is predicted mainly on the distribution of the hydrocarbon products (6–9), kinetic studies of skeletal rear-

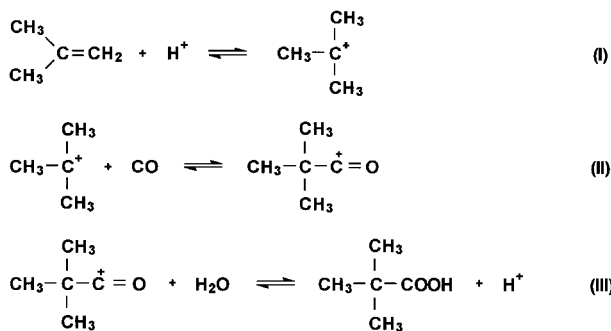
rangement of olefins (10), and scrambling of the  $^2\text{H}$  and  $^{13}\text{C}$  labels in model reactions over solid acids (11–22). Only very stable triphenylmethyl (11) and cyclopentenyl cations (22–24) were identified with  $^{13}\text{C}$  solid state NMR, more reactive alkyl carbenium ions (e.g., *tert*-butyl carbenium ion, TBCI) were not detected spectroscopically on solid acids. Due to the failure of numerous attempts to detect alkyl carbenium ions spectroscopically, it has been suggested that such cations are not formed in zeolites, and reactive intermediates represent alkoxy species (25). The latter can exhibit carbenium ion properties at high temperature under vibrational excitation and elongation of the C–O bond (25).

In addition to convincing spectroscopic data by Olah *et al.* (3–5), yet another evidence for the existence of carbenium ions in superacidic solutions as rather stable species comes from their ability to provide as intermediates to the classical Koch reaction (26) between olefins or alcohols and CO in the presence of water. Indeed, a generally accepted mechanism of Koch reaction includes three stages (Scheme 1) (27). First, an intermediate carbenium ion is formed by protonation of an olefin (stage I). Subsequent addition of CO to the carbenium ion gives rise to the acylium cation (oxocarbenium ions, stage II). The latter reacts with water to form the carboxylic acid, releasing the active proton of catalyst (stage III). Note that the ability of carbon monoxide to interact with carbenium ions in acidic media to give more stable acylium cations was reliably established by Hogeveen *et al.* (28).

Recently, experimental evidences were obtained (mainly by observing the scrambling of  $^{13}\text{C}$  and  $^2\text{H}$  labels with NMR) that intermediates with alkyl carbenium ion properties are formed on zeolites at low temperature (300 K) in the course of *tert*-butyl alcohol dehydration (17, 22) or isobutene conversion (15). There was also shown that octene-1, when adsorbed on H-ZSM-5 zeolite, also exhibits carbenium ion properties at 296 K (19).

\* To whom correspondence should be addressed.

† Deceased.



SCHEME 1

If carbenium ions are really formed from light olefins inside zeolites at room temperature, then according to Scheme 1 (27) they should interact with CO and convert the olefins or alcohols into carboxylic acids in the presence of water.

The above-mentioned experimental findings on the scrambling of  $^{13}\text{C}$  and  $^2\text{H}$  labels in alcohols and olefins on zeolites at low temperature (15, 17, 22), as well as the property of carbon monoxide to interact with carbenium ions in acidic media (28) prompted us to try to trap the intermediate alkyl carbenium ions (presumably formed from olefins and alcohols on H-ZSM-5) chemically with CO. One could expect that the reactions would proceed at low temperature, namely, at the temperature of alcohol dehydration or olefin oligomerization, where a generation of carbenium ions from alcohol (olefin) is expected on zeolite. In this case the formation of carboxylic acid as reaction product would serve as evidence for the formation of alkyl carbenium ion inside zeolite at low temperature. The other aim of this work was to further substantiate the possibility of Koch type reaction on zeolites under mild conditions. (Preliminary results on the observation of the Koch reaction under mild conditions on H-ZSM-5 have already been reported, see (29).)

Solid state  $^{13}\text{C}$  NMR spectroscopy was chosen as the main instrumental method for our study. It allowed us to monitor *in situ* both the transformations of the reagents and the formation of the reaction products in the course of the reaction. To facilitate NMR analysis and to attribute the observed NMR signals more reliably, the reagents (alcohols, olefins, and CO) labeled selectively with  $^{13}\text{C}$  isotope were used.

## 2. EXPERIMENTAL

**Samples preparation.** Zeolite H-ZSM-5 (Si/Al = 49) was synthesized according to Ref. (30) and characterized with X-ray powder diffraction analysis and chemical analysis. Approximately 0.3 g of zeolite was loaded into a 10-mm o.d. glass tube and then heated at 723 K for 1.5 h in air to remove atmospheric moisture and for 4 h under vac-

uum at  $10^{-5}$  Torr (1 Torr =  $133.3 \text{ N m}^{-2}$ ). After cooling the sample to ambient temperature (296 K), we froze out equal amounts (300–350  $\mu\text{mol/g}$ ) of butyl alcohol and CO or olefin, CO and  $\text{H}_2\text{O}$  on H-ZSM-5 under vacuum at the temperature of liquid nitrogen, and the glass tube with the zeolite was then sealed off from the vacuum system. Further, the sample was slowly warmed and kept at 296 K for a few hours or heated for a certain period of time at 373 K to accelerate the reaction.

**Analysis of reaction products.** The reaction products were analyzed directly inside the zeolite pores with *in situ*  $^{13}\text{C}$  NMR. An extent of alcohol or olefin conversion into carboxylic acid was estimated from the comparison of the  $^{13}\text{C}$  NMR signal intensities of the initial alcohol (olefin) and final carboxylic acid. To confirm our conclusions on the organic products formed, we also made several *ex situ* GC-MS experiments. The zeolite sample was dissolved in 10% NaOH solution. The solution that formed was neutralized with  $\text{H}_2\text{SO}_4$ , and the organic products were extracted with  $\text{Et}_2\text{O}$ . After subsequent evaporation of  $\text{Et}_2\text{O}$ , GC-MS analysis was made.

To facilitate NMR analysis, alcohols, olefins, and CO with selective  $^{13}\text{C}$  labels (82–92%  $^{13}\text{C}$  isotope enrichment) were employed.

Before *in situ* NMR analysis, in most of our experiments the glass tube with the zeolite sample was opened and the zeolite sample with adsorbed reaction products was transferred under air into a 7 mm zirconia NMR rotor for NMR experiment (*vide infra*). We have also carried out some NMR experiments, where air with atmospheric moisture was not permitted to the zeolite sample. For this purpose ca. 0.1 g of zeolite was placed into a glass tube which, after sealing off from the vacuum line, could be tightly packed into a zirconia rotor. We have not found any difference between NMR spectra for the samples, recorded in opened or sealed tubes.

**$^{13}\text{C}$  NMR experiments.**  $^{13}\text{C}$  NMR spectra with high power proton decoupling, magic angle spinning (MAS), and with or without cross-polarization (CP), denoted below as  $^{13}\text{C}$  CP/MAS NMR or  $^{13}\text{C}$  MAS NMR, were recorded at 100.613 MHz (magnetic field of 9.4 Tesla) on a Bruker MSL-400 spectrometer at 296 K. The following conditions were used for recording spectra with CP: the proton high power decoupling field was 11.7 G (5.0  $\mu\text{s}$   $90^\circ$  H pulse), contact time 5 ms at Hartmann-Hahn matching conditions 50 kHz, delay time between scans 3 s, spinning rate 2.4–3.2 kHz. Number of scans was 600–20000.

In order to make quantitative estimations of the signal areas, one pulse excitation MAS spectra were recorded with  $45^\circ$  flip angle  $^{13}\text{C}$  pulses of 2.5  $\mu\text{s}$  duration and 10–15 s recycle delay, which satisfied a  $10T_1$  condition. High power proton decoupling in these experiments was used only during the acquisition time. This eliminates Nuclear Overhauser

Enhancement of the signal areas and allows quantitative assessment of the signal areas (31).

$^{13}\text{C}$  chemical shifts for carbon nuclei of adsorbed organic species were measured with respect to TMS as the external reference with accuracy  $\pm 0.5$  ppm. Precision in the determination of the relative line position was 0.1–0.15 ppm.

The temperature of the samples was controlled with a BVT-1000 variable-temperature unit.

**GC-MS analysis.** The fused silica capillary column of 35 m  $\times$  0.3 mm i.d. with OV-101 as the active phase, forming a film of 0.3  $\mu\text{m}$  thickness, was used in this study. Temperature was programmed from 50°C (2 min) to 280°C at 8°C/min rate. The detector was a mass spectrometer (VG 70-70), which was scanned from  $m/e=20$  to  $m/e=600$  at a cycle time of 4 s.

### 3. RESULTS AND DISCUSSION

#### 3.1. Formation of Carboxylic Acids via Trapping of Carbenium Ions Generated from Butyl Alcohols

**tert-Butyl alcohol.** *tert*-Butyl alcohol undergoes dehydration (13, 14) and generates the *tert*-butyl carbenium (TBCI) ion on zeolite H-ZSM-5 at room temperature (17, 22). Therefore, the interaction of TBCI with carbon monoxide followed by the formation of the corresponding carboxylic acid was expected to occur also at room temperature.

$^{13}\text{C}$  CP/MAS NMR spectra recorded after coadsorption of *t*-BuOH and CO on H-ZSM-5, are presented in Fig. 1. When taken together, these spectra can easily be rationalized in terms of formation of the trimethylacetic acid (TMAA) as the main reaction product. Indeed, if we use for coadsorption  $[2-^{13}\text{C}]t\text{-BuOH}$  (i.e., the alcohol labeled in the quaternary carbon atom) and the unlabeled CO, then two signals at 40.7 and 81.4 ppm dominate (Fig. 1A). The appearance of the signal at 40.7 ppm is well understood, provided that adsorbed  $[2-^{13}\text{C}]t\text{-BuOH}$  reacts with CO, as shown in Scheme 2. According to Scheme 2, mainly the signal from the  $^{13}\text{C}$  labeled quaternary carbon atom of TMAA should be observed. Indeed, there is a good agreement between the chemical shift for the signal at 40.7 ppm in Fig. 1A and that for the signal of the quaternary carbon atom in liquid TMAA [38.5 ppm (32)]. The signal at 81.4 ppm, which

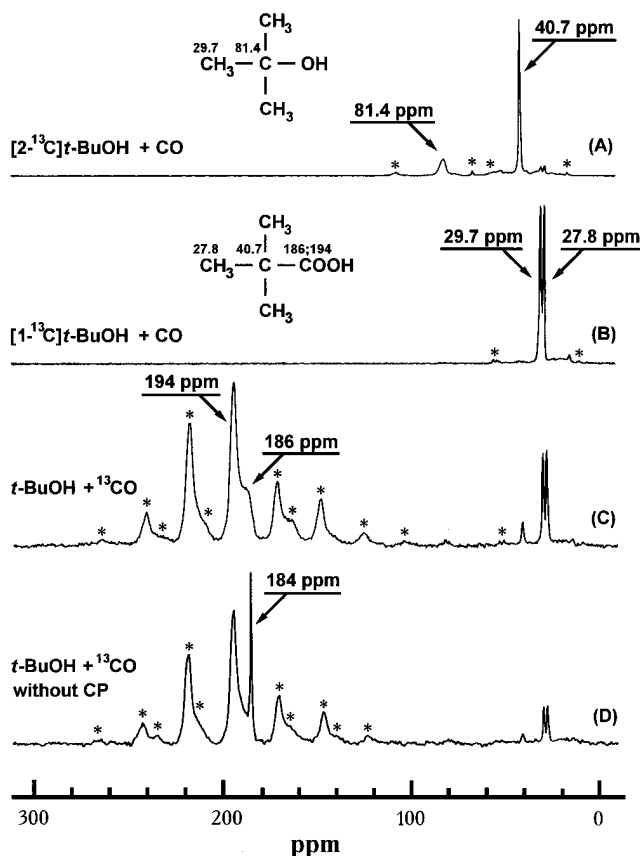
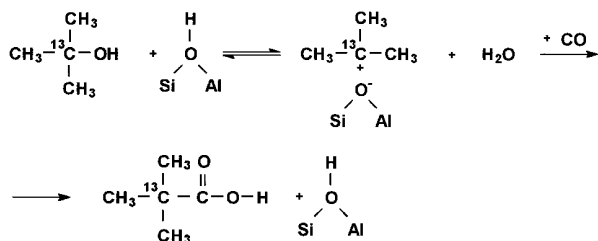


**FIG. 1.**  $^{13}\text{C}$  CP/MAS NMR spectra for the products formed after coadsorption of *t*-BuOH and CO on H-ZSM-5 zeolite at 296 K: (A) Coadsorption of the *t*-BuOH,  $^{13}\text{C}$ -labeled in the quaternary carbon atom (82%  $^{13}\text{C}$  enrichment), and unlabeled CO. (B) Coadsorption of the *t*-BuOH, labeled with  $^{13}\text{C}$  in a methyl group (67%  $^{13}\text{C}$  enrichment) and unlabeled CO. (C) Coadsorption of the  $^{13}\text{C}$ -labeled CO (90%  $^{13}\text{C}$  enrichment) and unlabeled *t*-BuOH. (D) One pulse excitation  $^{13}\text{C}$  MAS NMR spectrum with high-power proton decoupling, recorded after coadsorption of the  $^{13}\text{C}$  and unlabeled *t*-BuOH. This spectrum corresponds to the spectrum (C) but was recorded without cross-polarization. In each case, 300  $\mu\text{mol/g}$  of *t*-BuOH and CO (or  $^{13}\text{C}$ ) were adsorbed; 6000 scans were collected for (A), 3000 scans for (B), 16000 scans for (C), 2200 scans for (D). Asterisks (\*) denote spinning side bands.  $^{13}\text{C}$  chemical shifts for adsorbed initial alcohols and the formed carboxylic acids are given above each molecule depicted in Figs. 1–5.

is typical for *tert*-butyl group bound to oxygen, should be attributed to unreacted alcohol because its chemical shift and line width are indeed very close to those for quaternary carbon atom in *t*-BuOH adsorbed on H-ZSM-5 (17, 22).

One of the two signals, observed for coadsorption of *t*-BuOH, labeled with  $^{13}\text{C}$  in a methyl group ( $[1-^{13}\text{C}]t\text{-BuOH}$ ) and the unlabeled CO, namely, the signal at 27.8 ppm (Fig. 1B), further supports the conclusion on the formation of TMAA. Indeed, methyl groups of liquid TMAA exhibit the signal at 27.8 ppm (32). The second signal at 29.7 ppm belongs to the unreacted alcohol (17, 22).

When the labeled  $^{13}\text{C}$  and unlabeled *t*-BuOH is used, we observe basically two signals at 194 and 186 ppm, the



**SCHEME 2**

latter being seen as a shoulder of the former one (Fig. 1C). These two signals are in the region typical for carbonyl groups (33); however, their positions and line shapes with numerous spinning side bands differ from that for the earlier reported signal at 184 ppm of  $^{13}\text{C}$  adsorbed on H-ZSM-5 (34). We have also observed the narrow line at 184 ppm (without spinning side bands) from unreacted  $^{13}\text{C}$  in the spectrum recorded without cross-polarization (Fig. 1D). Thus, two signals appear in the region, where a single signal from the  $-\text{COOH}$  group of TMAA is expected (185.7 ppm in liquid TMAA (32)). Both these signals certainly belong in TMAA, because TMAA specially adsorbed on H-ZSM-5 in a separate experiment (spectrum is not shown) exhibits the same two signals at 194 and 186 ppm, in addition to the signals at 40.7 and 27.8 ppm from the quaternary carbon atom and  $\text{CH}_3$  groups, respectively. From our NMR data we cannot attribute unambiguously these two signals to some certain states of adsorbed TMAA. Nevertheless, a tentative assignment can be made. Usually, more acidic bridged  $\text{Si}-\text{OH}-\text{Al}$  groups produce larger perturbation on  $^{13}\text{C}$  chemical shifts of adsorbed molecules (35, 36) compared to less acidic  $\text{Si}-\text{OH}$  groups (36). Therefore, the signal at 194 ppm may belong to TMAA adsorbed on bridged  $\text{Si}-\text{OH}-\text{Al}$  groups, while the signal at 186 ppm may be assigned to TMAA adsorbed on terminal  $\text{Si}-\text{OH}$  groups. However, other possibilities may be that these two signals belong to monomeric and dimeric states of TMAA (37) inside H-ZSM-5 or to TMAA adsorbed on  $\text{Si}-\text{OH}-\text{Al}$  groups with different spatial surroundings inside the zeolite framework.

Relatively weak signals at 27.8, 40.7, and 29.7 ppm (Fig. 1C) belong to  $^{13}\text{C}$  atoms that are present in natural abundance in adsorbed TMAA and *t*-BuOH molecules, respectively.

To confirm the formation of TMAA inside H-ZSM-5 zeolite, we have carried out GC-MS analysis of the residue formed after dissolving the zeolite sample in 10% NaOH solution and extraction of organic products with  $\text{Et}_2\text{O}$ . GC-MS analysis supported our NMR data and showed that TMAA was the main reaction product.

Thus, our experiments clearly indicate that TBCI generated from *t*-BuOH on H-ZSM-5 is easily trapped with CO at room temperature, similar to the trapping of carbenium ions in classical Koch synthesis (26–28) or in carbonylation of alkanes in liquid superacids (38).

The conversion of *t*-BuOH into TMAA after the retention of the zeolite sample with coadsorbed *t*-BuOH and CO for a few hours at 296 K was about 50%. Retaining the zeolite sample for a few days at 296 K resulted in 100% conversion of the alcohol into the acid. At 373 K a complete conversion of the alcohol occurred within 10 min.

Note that when *t*-BuOH and CO are coadsorbed on H-ZSM-5,  $^{13}\text{C}$  labels do not undergo scrambling over the carbon skeleton of the reaction participants, as they

do when *t*-BuOH is adsorbed on H-ZSM-5 without CO (14, 17, 22). Moreover, no signals appear at 10–40 ppm from isobutene oligomers, which are formed from *t*-BuOH on H-ZSM-5 in the absence of CO (14, 17, 22, 39). Both these facts show that interaction of CO with TBCI, generated from *t*-BuOH, is a faster process than the  $^{13}\text{C}$  scrambling or isobutene oligomerization.

Note that the observed high conversion of the alcohol into the acid is achieved at low temperature and without using excess CO. This fact opens up new possibilities for the accomplishment of the Koch reaction on zeolites under very mild conditions, rather than under severe conditions as reported by Hoelderich *et al.* (40).

*iso-Butyl alcohol.* *iso*-Butyl alcohol does not undergo any noticeable transformations on H-ZSM-5 at 296 K. At 373 K the dehydration of *i*-BuOH proceeds with a notable rate (41). At 373 K, under the reaction conditions used in this study, it is completed within one hour to give isobutylsilyl ether (IBSE, a stable alkoxy intermediate) and water (16, 18). However, a small amount of carbenium ions is claimed to be in equilibrium with IBSE (16, 18). These carbenium ions generated at 373 K, may interact with CO.

$^{13}\text{C}$  CP/MAS NMR spectra, recorded after coadsorption of *i*-BuOH and CO on H-ZSM-5 are given in Fig. 2. After coadsorption of  $^{13}\text{C}$  and unlabeled *i*-BuOH and subsequent heating of the sample at 373 K for 1 h, the observed spectrum is identical to that recorded after coadsorption of *i*-BuOH and  $^{13}\text{C}$  (compare Figs. 1C and 2A). The identity of these two spectra indicates that trimethylacetic acid is formed from *i*-BuOH and CO.

When *i*-BuOH selectively labeled with  $^{13}\text{C}$  in the  $\text{CH}_2-\text{OH}$  group ( $[1-^{13}\text{C}]\text{i}$ -BuOH) and unlabeled CO were coadsorbed on the zeolite and heated for 1 h at 373 K, the labeled  $\text{CH}_2-\text{OH}$  group is transformed into the labeled  $\text{CH}_3$  group of TMAA. A selective transformation of the signal at 72.3 ppm from the labeled  $\text{CH}_2\text{OH}$  group of the unreacted alcohol (Fig. 2B) into the signal at 27.8 ppm from the methyl group of TMAA after completing the reaction at 373 K (Fig. 2C) further supports the conclusion for the formation of TMAA. Comparison (in the  $^{13}\text{C}$  MAS NMR spectrum recorded without CP) of the intensities of the signals from the  $^{13}\text{CH}_2\text{OH}$  group of the unreacted alcohol and from the  $^{13}\text{CH}_2\text{OH}$  transformed into the methyl group of the acid, allows us to conclude that more than 70% of the alcohol is converted into TMAA upon heating at 373 K for 1 h.

In principle, an interaction of carbenium ions, formed from *i*-BuOH, with CO can result in the formation of both trimethylacetic acid and isovaleric acid (ISVA) (see Scheme 3). Selective transformation of the labeled  $^{13}\text{CH}_2\text{OH}$  group of the alcohol into the methyl group of TMAA, rather than into the  $^{13}\text{CH}_2\text{COOH}$  group of ISVA (in the latter case a signal at 44.1 ppm from the  $^{13}\text{CH}_2\text{COOH}$  (42) group should be observed instead of the signal at

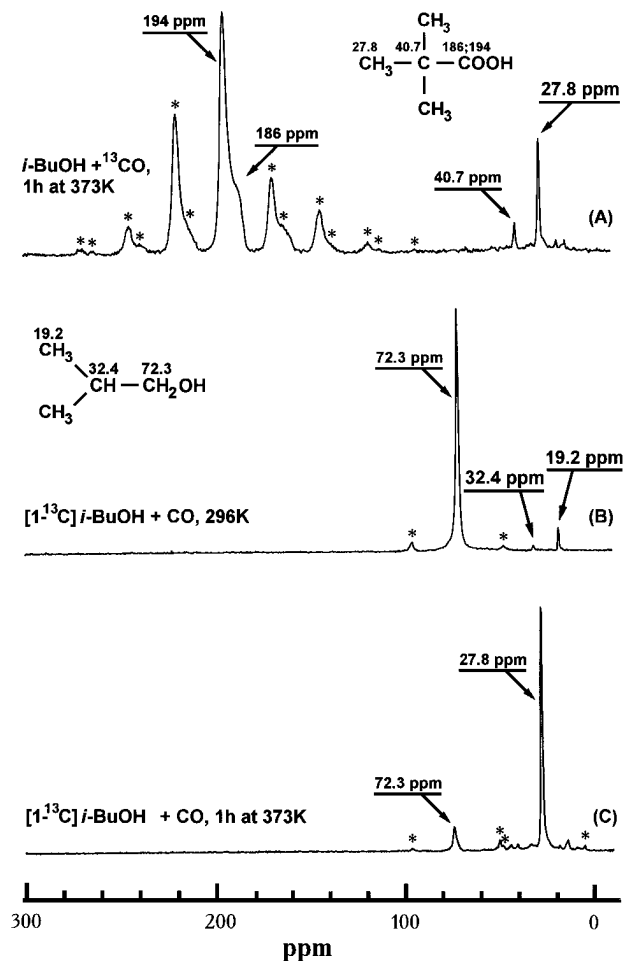


**FIG. 2.**  $^{13}\text{C}$  CP/MAS NMR spectra for the products formed after coadsorption of *i*-BuOH and CO on H-ZSM-5 zeolite at 296 K: (A) Coadsorption of the unlabeled *i*-BuOH and  $^{13}\text{C}$ -labeled CO (90%  $^{13}\text{C}$  enrichment); the sample was further heated at 373 K for 1 h. (B) Adsorption of the *i*-BuOH, labeled with  $^{13}\text{C}$  in the  $\text{CH}_2\text{OH}$  group (82%  $^{13}\text{C}$  enrichment) without CO. (C) Coadsorption of the *i*-BuOH, labeled with  $^{13}\text{C}$  in the  $\text{CH}_2\text{OH}$  group (82%  $^{13}\text{C}$  enrichment) and unlabeled CO with subsequent heating at 373 K for 1 h. In each case, 300  $\mu\text{mol/g}$  of *i*-BuOH and CO (or  $^{13}\text{C}$ ) were adsorbed; 18000 scans were collected for (A), 2000 scans for (B), 2000 scans for (C). Asterisks (\*) denote spinning side bands.

27.8 ppm), indicates that among the supposed (16, 18) family of butyl carbenium ions generated from *i*-BuOH on H-ZSM-5, CO interacts mainly with the *t*-butyl one (TBCI).

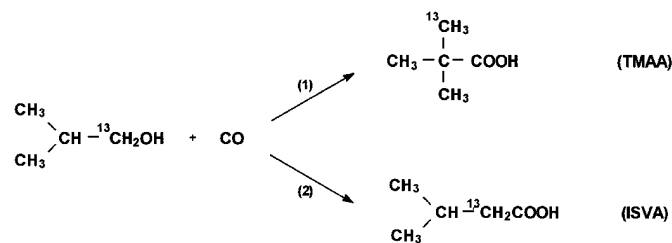
This means that hydrogen transfer, which produces TBCI from initially formed isobutyl carbenium ion (18), occurs much faster than interaction of isobutyl carbenium ion with CO. Otherwise, preferential formation of ISVA would be expected. Note also, that the rate of IBSE formation from the alcohol exceeds the rate of intramolecular transfer of hydrogen in the isobutyl cation. Otherwise, *tert*-butyl silyl ether (TBSE) would have been formed from *i*-BuOH on H-ZSM-5 in the absence of CO, which in reality had not been observed (16, 18).

***n*-Butyl alcohol.** *n*-Butyl alcohol, similar to *i*-BuOH, does not transform on H-ZSM-5 at room temperature. However, it is slowly dehydrated at 373 K (43, 44). Hence, trapping of carbenium ions (which may be generated from *n*-BuOH at 373 K) with CO can also lead to the formation of a carboxylic acid.

Figure 3 shows  $^{13}\text{C}$  CP/MAS NMR spectra recorded after coadsorption of *n*-BuOH and CO on H-ZSM-5 and heating for a few hours at 373 K. In the case of coadsorption of labeled  $^{13}\text{C}$  and unlabeled alcohol, the signals at 186–194 ppm (similar to the case with both *t*-BuOH and *i*-BuOH) evidence for the formation of a carboxylic acid (Fig. 3A). If unlabeled CO and *n*-BuOH, labeled in the  $\text{CH}_2\text{OH}$  group ( $[1-^{13}\text{C}]n\text{-BuOH}$ ), are employed, the following signals are observed in the spectrum (Fig. 3B): (1) the most intense signal from the labeled  $^{13}\text{CH}_2\text{OH}$  fragment of the unreacted alcohol at 68.5 ppm (44); (2) the signal at 76.3 ppm from the labeled  $^{-13}\text{CH}_2\text{-O-}$  group of di-*n*-butyl ether (*n*-Bu $_2$ O), formed from the alcohol (44); (3) two intense signals at 11.6 and 16.8 ppm, which presumably belong to some labeled  $^{13}\text{CH}_3$  groups of reaction products (*vide infra*); (4) the less intense signals from the rest unlabeled  $\text{CH}_2$  and  $\text{CH}_3$  groups of *n*-BuOH, *n*-Bu $_2$ O, and the products of butene oligomerization are seen between 10 and ca. 40 ppm (44).

The signals at 68.5 and 76.3 ppm remain in the spectrum after heating of the zeolite sample at 373 K for 15 h, which indicates that dehydration is not completed even for this time interval (Fig. 3C). Note also, that such long heating results in the growth of the signals from butene oligomers at 14–40 ppm (44).

Appearance of the two relatively intense signals at 11.6 and 16.8 ppm can be rationalized in terms of the reactions presented in Scheme 4. Indeed, the scrambling of the label in butyl carbenium ion by means of hydride shift reactions, followed by the reactions of the two differently labeled secondary butyl carbenium ions with CO and  $\text{H}_2\text{O}$ , will lead to the appearance of two intense signals in the  $^{13}\text{C}$  NMR spectrum attributed to two labeled methyl groups of the 2-methyl-butyric acid, MBA (see Scheme 4). Indeed, the chemical shifts for two intense signals at 11.6 and 16.8 ppm in Fig. 3B coincide with those shifts for the methyl groups in MBA (45).



**SCHEME 3**

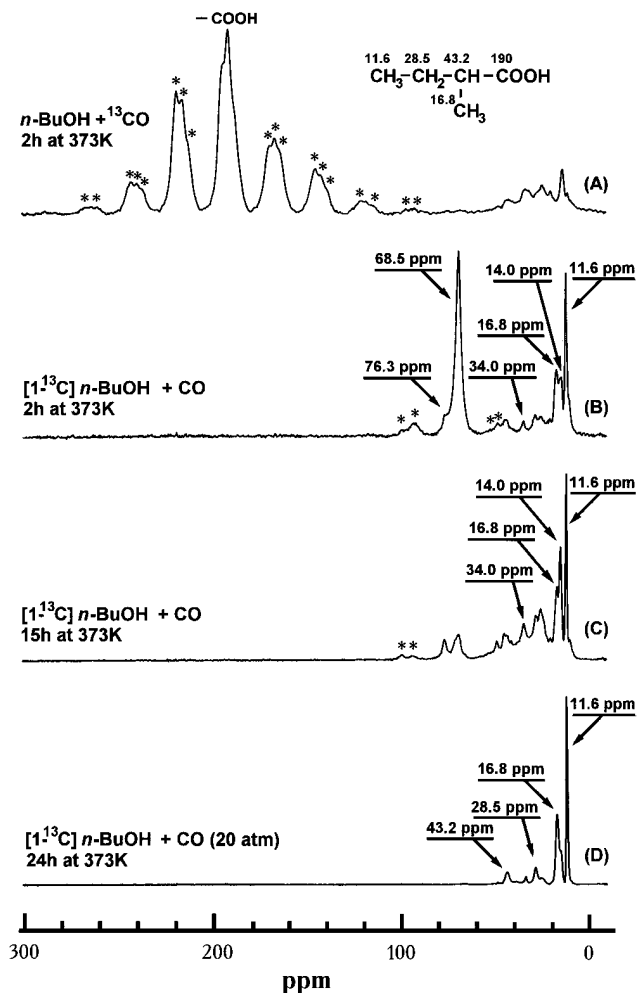


**FIG. 3.**  $^{13}\text{C}$  CP/MAS NMR spectra for the products formed after coadsorption of *n*-BuOH and CO on H-ZSM-5 zeolite at 296 K: (A) Coadsorption of the unlabeled *n*-BuOH and  $^{13}\text{C}$ -labeled CO (90%  $^{13}\text{C}$  enrichment); the sample was further heated at 373 K for 2 h. (B) Coadsorption of the *n*-BuOH, labeled with  $^{13}\text{C}$  in the  $\text{CH}_2\text{OH}$  group (82%  $^{13}\text{C}$  enrichment) and unlabeled CO with subsequent heating at 373 K for 2 h. (C) as sample (B) but heated for 15 h at 373 K. (D) as sample (B) but heated at 373 K for 24 h under 20 atm pressure of CO. In each case, 300  $\mu\text{mol/g}$  of *n*-BuOH and CO (or  $^{13}\text{C}$ CO) were adsorbed; 18000 scans have been collected for (A), 2000 scans for (B), 4000 scans for (C), 4000 scans for (D). Asterisks (\*) denote spinning side bands.

Thus, mainly a secondary acid is synthesized from the primary alcohol. However, a small amount of the primary valeric acid (VA) is also formed. In case of its formation, the label from *n*-BuOH should penetrate into the  $\text{CH}_3$  and  $-\text{CH}_2\text{COOH}$  groups of the VA, the signals from which must be located near 14 and 34 ppm, respectively (46). Both signals are clearly seen in the spectra of Figs. 3B–3D. However, while we attribute the small signal at 34.0 ppm solely to VA, the more intense signal at 14.0 ppm seems to have a contribution also from butene oligomers, at least in the spectra of Figs. 3B and 3C.

Comparison of the intensities of the signals from MBA and VA in  $^{13}\text{C}$  MAS NMR spectra recorded without CP indicates that the primary acid is formed in a few percent of the amount of MBA only. Such distribution between the quantities of the two acids can be explained by a larger stability of secondary carbenium ions compared to primary ones.

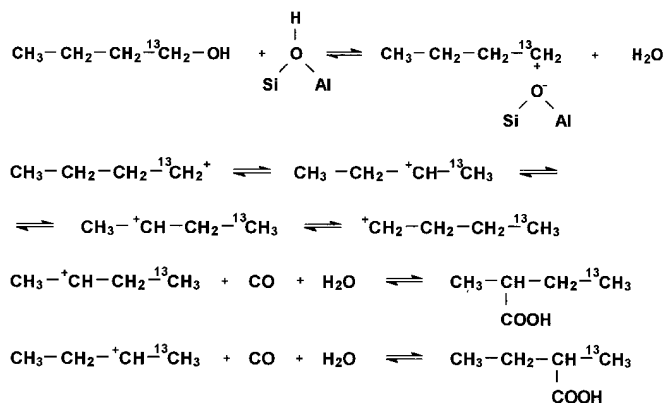
Upon long heating (24 h) of  $[1-^{13}\text{C}]n\text{-BuOH}$  on the zeolite under pressurized conditions (20 atm of CO), the following signals are observed in the  $^{13}\text{C}$  NMR spectrum: intense signals from MBA at 11.6, 16.8, 28.5, and 43.2 ppm (45) and weak ones from VA at  $\sim 14, 22\text{--}27, 34.0$  ppm (46). The signals from *n*-Bu $_2$ O and butene oligomers are not observed in this case (Fig. 3D).

Thus,  $^{13}\text{C}$  solid state NMR data evidence that carbenium ions formed in the course of *n*-BuOH dehydration on H-ZSM-5 at 373 K can be trapped with CO to form carboxylic acids. The trapping of carbenium ions proceeds even without application of pressurized conditions. However, in this case by-products—*n*-Bu $_2$ O and butene oligomers—are also formed.

The use of excess CO prevents the formation of these by-products. In this case both the secondary and primary acids are formed, the ratio between them apparently being defined by the relative stabilities of the secondary and primary butyl cations in the zeolite pores.

### 3.2. Formation of Carboxylic Acids via Trapping of Carbenium Ions Generated from Olefins

We have already mentioned that similar to alcohols, olefins can also form carboxylic acids upon carbonylation in the presence of water both in liquid acids and on solid ones. However, these reactions usually proceed only under high pressure and temperature conditions (27). At the same time, it is well known that small olefins ( $\text{C}_2\text{--}\text{C}_4$ ) oligomerize on acidic form zeolites at ambient temperature (see, e.g., Ref. (47)). Oligomerization is assumed to proceed via formation of carbenium ions (47). If this suggestion is true, then



**SCHEME 4**

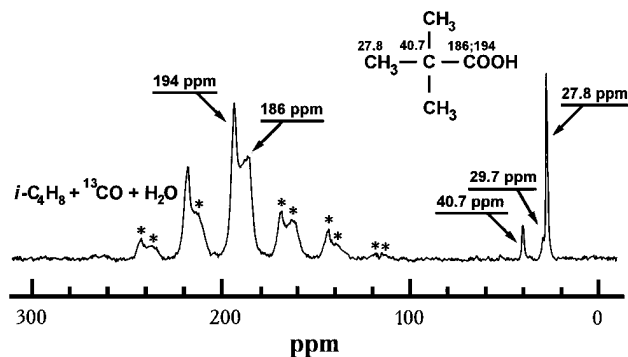


**FIG. 4.**  $^{13}\text{C}$  CP/MAS NMR spectrum for the products formed after coadsorption of unlabeled isobutene,  $^{13}\text{C}$ -labeled CO (90%  $^{13}\text{C}$  enrichment), and water on H-ZSM-5 zeolite at 296 K. 300  $\mu\text{mol/g}$  of isobutene,  $^{13}\text{C}$ CO, and  $\text{H}_2\text{O}$  were adsorbed; 20000 scans have been collected. Asterisks (\*) denote spinning side bands.

one can try, similar to the case with alcohols, to trap these cations at room temperature and normal pressure with carbon monoxide to form ultimately carboxylic acids in the presence of water (see Scheme 1).

*iso-Butene.* Figure 4 shows  $^{13}\text{C}$  CP/MAS NMR spectrum recorded after coadsorption of unlabeled isobutene,  $i\text{-C}_4\text{H}_8$ ,  $^{13}\text{C}$ CO, and  $\text{H}_2\text{O}$  in equal amounts on H-ZSM-5 at 296 K. Comparison of the spectrum in Fig. 4 with the spectra recorded after coadsorption of  $^{13}\text{C}$ CO and unlabeled  $t\text{-BuOH}$  or  $i\text{-BuOH}$  (Figs. 1C and 2A) shows the strong similarity of these spectra, i.e., points to the formation of trimethylacetic acid (TMAA) from  $i\text{-C}_4\text{H}_8$  at room temperature. Note that in the spectrum of Fig. 4 the signals between 10 and 40 ppm from the expected butene oligomers (17) are not observed, the main signals at 27.8, 40.7 and 186, 194 ppm are arising from TMAA (32).

This fact indicates that interaction of TBCI (generated from  $i\text{-C}_4\text{H}_8$ ) with CO is faster than the interaction of this cation with another olefin molecule (similar to the case with TBCI, formed from  $t\text{-BuOH}$ ).

A weak signal at 29.7 ppm (seen as a shoulder of the signal at 27.8 ppm) may be attributed to the unlabeled  $\text{CH}_3$  groups of  $t\text{-BuOH}$ , formed as a result of  $i\text{-C}_4\text{H}_8$  hydration (48). No signals are observed from the initial olefin. Comparison of the signal intensities from the methyl groups of  $t\text{-BuOH}$  and TMAA in the one pulse excitation spectrum recorded without CP allowed us to estimate the olefin conversion into TMAA to be no less than 80%, while that into  $t\text{-BuOH}$  should not exceed 20%.

Thus, *tert*-butyl cation is formed from  $i\text{-C}_4\text{H}_8$  on H-ZSM-5 at 296 K and easily trapped with CO, forming TMAA in the presence of  $\text{H}_2\text{O}$ .

*Ethene.* Ethene easily oligomerizes on H-ZSM-5 at room temperature (see, e.g., Ref. (47) and references cited therein). It is assumed that ethyl cation  $\text{CH}_3\text{CH}_2^+$  is formed initially from ethene after its adsorption on the zeolite. Fur-

ther, ethyl cation interacts with another ethene molecule to give butyl cation. Subsequent interaction of the latter cation with ethene molecule gives rise to hexyl cation, and so on.

In the case of coadsorption of CO,  $\text{H}_2\text{O}$ , and  $\text{C}_2\text{H}_4$  on H-ZSM-5 one could expect either ethene oligomerization or its carbonylation to prevail, depending on whether the expected ethyl cation would react faster with another ethene molecule or with CO molecule. In the former case, oligomerization would be observed, while in the latter case propionic acid would be formed. Oligomers might give also carboxylic acids with longer aliphatic fragments.

Figure 5A shows  $^{13}\text{C}$  CP/MAS NMR spectrum recorded after coadsorption of unlabeled  $\text{C}_2\text{H}_4$ ,  $^{13}\text{C}$ CO, and  $\text{H}_2\text{O}$  on H-ZSM-5 at 296 K. Intense signals at 188–196 ppm (33) point to the formation of a carboxylic acid. The signal at 125 ppm belongs to the unreacted ethene with the natural abundance of  $^{13}\text{C}$  isotope (49). When unlabeled CO and  $^{13}\text{C}$ -labeled ethene ( $^{13}\text{CH}_2=\text{CH}_2$ ) are used for coadsorption, four signals between 8 and 50 ppm are clearly seen in the  $^{13}\text{C}$  CP/MAS NMR spectrum (Fig. 5B). According to their chemical shifts, these signals belong to 2-methyl-2-ethyl-butyric acid (METBA) [(48.7 (C), 31.9 ( $\text{CH}_2$ ), 21.5 ( $\text{CH}_3$ ), 8.4 ( $\text{CH}_3$ ) ppm] (32). Conversion of ethene into

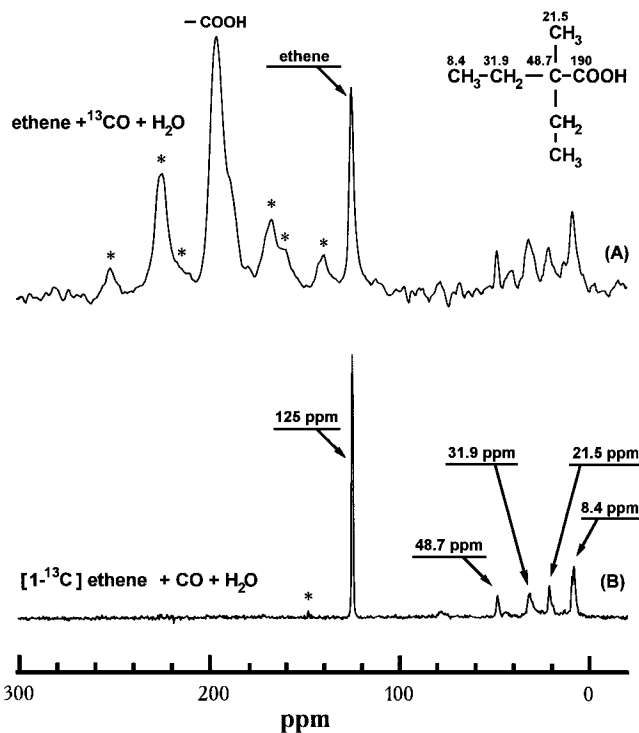


**FIG. 5.**  $^{13}\text{C}$  CP/MAS NMR spectra for the products formed after coadsorption of ethene, CO, and  $\text{H}_2\text{O}$  on H-ZSM-5 zeolite at 296 K: (A) Coadsorption of the unlabeled ethene and  $^{13}\text{C}$ -labeled CO (90%  $^{13}\text{C}$  enrichment). (B) Coadsorption of the ethene, labeled with  $^{13}\text{C}$  in one of the  $=\text{CH}_2$  groups (82%  $^{13}\text{C}$  enrichment) and unlabeled CO. In each case, 300  $\mu\text{mol/g}$  of ethene, CO (or  $^{13}\text{C}$ CO), and  $\text{H}_2\text{O}$  were adsorbed; 18000 scans have been collected for (A), 4000 scans for (B). Asterisks (\*) denote spinning side bands.

the acid is about 40% within a few hours, as estimated from the one pulse excitation  $^{13}\text{C}$  NMR spectrum recorded without CP.

Weak signals at 78 ppm as well as those at 30.5 ( $\text{CH}_2$ ), 19.5 ( $\text{CH}_3$ ), 9.4 ( $\text{CH}_3$ ) ppm according to their positions, may be attributed to an alcohol, e.g., 1-methyl-1-ethylpropanol (METPRA) (50, 51), formed upon the direct interaction of a water molecule with an alkyl carbenium ion  $(\text{CH}_3\text{CH}_2)_2^+\text{CCH}_3$ , rather than with acylium cation  $(\text{CH}_3\text{CH}_2)_2(\text{CH}_3)\text{C}^+\text{C}=\text{O}$ , from which the acid is formed.

Thus, ethene reacts at 296 K with CO and  $\text{H}_2\text{O}$  to give selectively METBA, rather than propionic or butyric acids, and long chain carboxylic acids are not formed. This fact indicates that initially formed ethyl cation reacts faster with another ethene molecule than with a CO molecule. The same is true for butyl cation formed in the former reaction. However, for hexyl cation the reaction with CO becomes faster than further oligomerization.

The selective formation of METBA in this reaction evidences for the proceeding of ethene oligomerization (at least up to  $\text{C}_6$  cation) inside narrow channels of H-ZSM-5 (52) according to the classic carbenium-ion mechanism like in acidic solutions: a primary formed ethyl cation interacts with another ethene molecule to give secondary butyl cation, interaction of the latter with ethene results in a tertiary hexyl cation. The most stable *t*-hexyl cation interacts with CO and water to form METBA.

It is interesting that selective formation of METBA from ethene was also observed in solutions containing  $(\text{H}_3\text{O}^+)(\text{BF}_4)^-$  as the catalyst (27). Thus, there exists a complete analogy between the behavior of this liquid acid catalyst and solid acid H-ZSM-5 zeolite catalyst in the reaction of ethene with CO and  $\text{H}_2\text{O}$ .

Finally, let us stress again a remarkable selectivity of CO in the trapping of tertiary  $\text{C}_6$  cation, rather than primary or secondary linear  $\text{C}_4$  cations. This provides the selective formation of METBA from ethene, CO and  $\text{H}_2\text{O}$  feedstock.

**Octene-1.** It was shown in Ref. (19) that alkyl carbenium ion is formed (though, perhaps in a small concentration) upon octene-1 adsorption on zeolite H-ZSM-5. We expected that similar to the cations generated from other olefins and alcohols (*vide supra*), this cation might be trapped with carbon monoxide to produce a carboxylic acid on the zeolite in the presence of water.

Figure 6 shows  $^{13}\text{C}$  CP/MAS NMR spectra, recorded after coadsorption of octene-1, CO and  $\text{H}_2\text{O}$  on H-ZSM-5. In the case of using  $^{13}\text{C}$ -labeled CO and unlabeled octene-1 (Fig. 6A), at least two overlapping intense signals with numerous spinning side bands are observed at 185–195 ppm. These signals point to the formation of one or several carboxylic acids.

Carbonylation of linear olefins with long hydrocarbon chains ( $\text{C}_{6+}$ ) in mineral acids produces usually tertiary carboxylic acids (27); e.g., octene-1 gives rise to a mix-

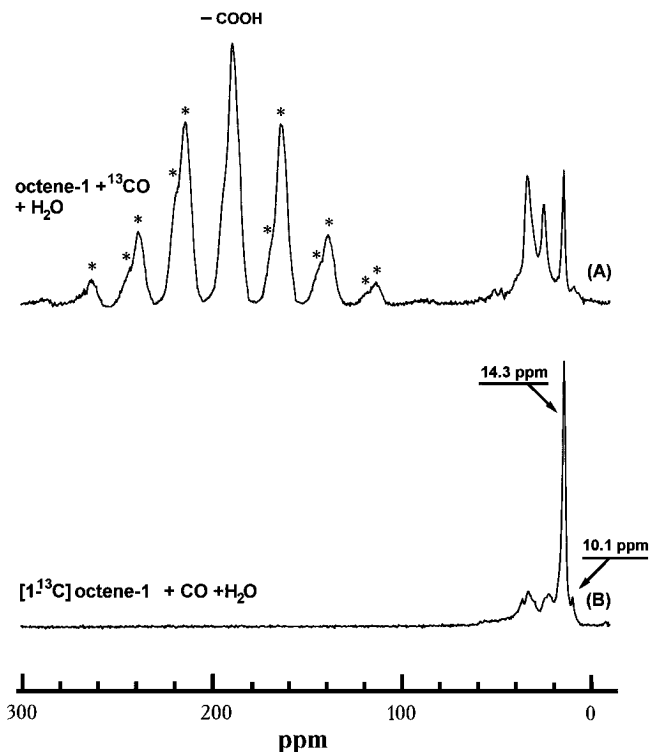
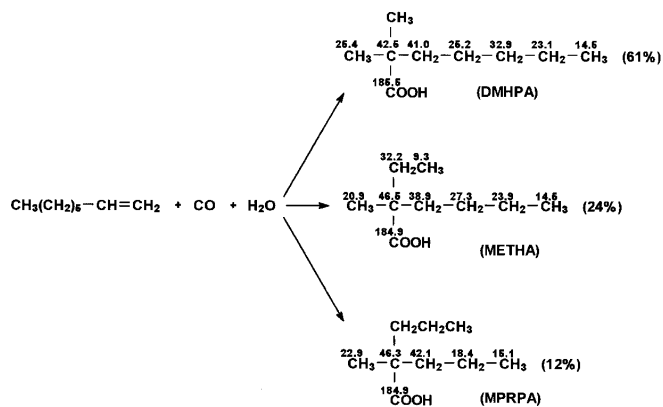


**FIG. 6.**  $^{13}\text{C}$  CP/MAS NMR spectra for the products formed after coadsorption of octene-1, CO and  $\text{H}_2\text{O}$  on H-ZSM-5 zeolite at 296 K: (A) Coadsorption of the unlabeled octene-1 and  $^{13}\text{C}$ -labeled CO (90%  $^{13}\text{C}$  enrichment). (B) Coadsorption of the octene-1, labeled with  $^{13}\text{C}$  in the terminal olefinic  $=\text{CH}_2$  group (82%  $^{13}\text{C}$  enrichment) and unlabeled CO. In each case, 300  $\mu\text{mol/g}$  of octene-1, CO (or  $^{13}\text{C}$ CO) and  $\text{H}_2\text{O}$  were adsorbed; 16000 scans have been collected for (A), 8000 scans for (B). Asterisks (\*) denote spinning side bands.

ture of 2,2-dimethyl-heptanoic acid (DMHPA), 2-methyl-2-ethyl-hexanoic acid (METHA), and 2-methyl-2-propyl-pentanoic acid (MPRPA) (27, 53) (see Scheme 5). This fact evidences for rearrangement of the linear olefin hydrocarbon skeleton into the branched ones during the reaction.

Preliminary analysis of the position of the signals at 10–40 ppm from aliphatic moieties (with the natural abundance of



**SCHEME 5**



$^{13}\text{C}$  isotope) (see Fig. 6A) of the acids formed from octene-1 evidences for the formation of carboxylic acids in H-ZSM-5 pores with linear, rather than highly branched hydrocarbon skeletons. Indeed, the signal at 14 ppm may belong to the terminal  $\text{CH}_3$  group in the linear fragment, the signal at 24 ppm to the  $\text{CH}_2$  group, which is next to the terminal  $\text{CH}_3$  group, the signal at 33 ppm to  $\text{CH}_2$  groups more remote from the terminal  $\text{CH}_3$  group (47, 54).

In the case of coadsorption of octene-1, selectively labeled with  $^{13}\text{C}$  in the terminal olefinic  $^{13}\text{CH}_2=$  group, unlabeled  $\text{CO}$  and  $\text{H}_2\text{O}$ , the signal at 14.3 ppm is preferentially observed (Fig. 6B). This experimental fact shows that no scrambling of the selective  $^{13}\text{C}$  label over octene-1 hydrocarbon skeleton occurs, as it does in the absence of  $\text{CO}$  (19). This means that  $\text{CO}$  interacts with the carbenium ion generated from octene-1 faster than the  $^{13}\text{C}$  label scrambles in this cation. The position of the intense signal in Fig. 6B indicates that it belongs to a methyl group of a linear  $\text{CH}_3\text{CH}_2(\text{CH}_2)_n$  fragment, where  $n \geq 1$ . A comparison of the chemical shifts in Fig. 6 with those for DMHPA, METHA, and MPRPA (32, 53) in solutions does not support their formation in the zeolite pores. According to the expected chemical shifts for DMHPA (Scheme 5,  $^{13}\text{C}$  shifts, presented above each carbon atom, are taken from Ref. (32)), the most intense signals corresponding to a sum of the methyl and methylene groups (chemical shifts of which in solution are 25.4 ( $2\text{CH}_3$ ), 25.2 ( $\text{CH}_2$ ), 23.1 ppm ( $\text{CH}_2$ )), should be observed at 23–25 ppm in the spectrum of Fig. 6A. In the case of the formation of METHA, intense signal at 9.3 ppm from the methyl group of the ethyl  $\text{CH}_3\text{CH}_2$  fragment would be observed in Fig. 6B together

with the signal at 14.3 ppm. If MPRPA were formed, there would be no signal at 33 ppm (32) in Fig. 6A. The chemical shifts of other tertiary carboxylic acids of the  $\text{C}_8\text{H}_{17}\text{COOH}$  family (32, 46) also do not fit the experimental spectra in Fig. 6.

To further elucidate the structure of the carboxylic acids formed inside the zeolite from octene-1, we followed a procedure already used (*vide supra*) to confirm the formation of trimethylacetic acid from *t*-BuOH in the zeolite pores. We dissolved the zeolite in  $\text{NaOH}$  solution and after its neutralization with  $\text{H}_2\text{SO}_4$ , extracted the organic products with  $\text{Et}_2\text{O}$ . Further, we analyzed these products with high resolution  $^{13}\text{C}$  NMR and GC-MS. For  $^{13}\text{C}$  NMR analysis,  $\text{Et}_2\text{O}$  was evaporated, and a residue was dissolved in  $\text{C}_6\text{D}_6$ . Then the  $^{13}\text{C}$  NMR spectrum was recorded (see Fig. 7). For GC-MS analysis,  $\text{Et}_2\text{O}$  solution of the organics extracted from the zeolite was treated with diazomethane ( $\text{CH}_2\text{N}_2$ ) in order to convert the acids into more volatile methyl esters of these acids. This procedure facilitates both gas chromatographic separation of the acids and analysis of the products on the basis of their *m/e* ratios (55).

Note the close similarity between the spectra of the reaction products trapped in the zeolite pores (Fig. 6) and those dissolved in  $\text{C}_6\text{D}_6$  (Fig. 7). The same two groups of signals dominate in both spectra, i.e., the lines around 185–195 ppm from carboxylic moieties and signals at 14.3–14.7, 23.5–24.0, 30–33 ppm from  $\text{CH}_3$  and  $\text{CH}_2$  moieties. But as expected, the signals in the solution spectrum are much more narrow than those in the solid zeolite. Therefore, the spectrum in Fig. 7 is more informative. From its analysis one can conclude that a mixture of carboxylic acids is extracted from the

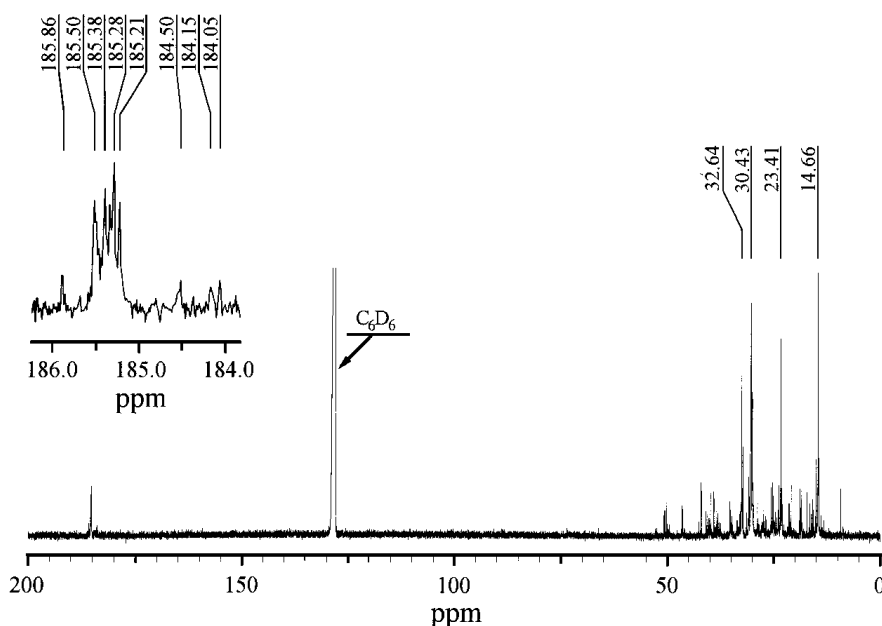


FIG. 7. High resolution  $^{13}\text{C}$  NMR spectrum for the organic products extracted after dissolving the zeolite H-ZSM-5 in 10%  $\text{NaOH}$  solution. The zeolite sample contained octene-1,  $\text{CO}$ , and  $\text{H}_2\text{O}$  coadsorbed in equal amounts at 296 K.

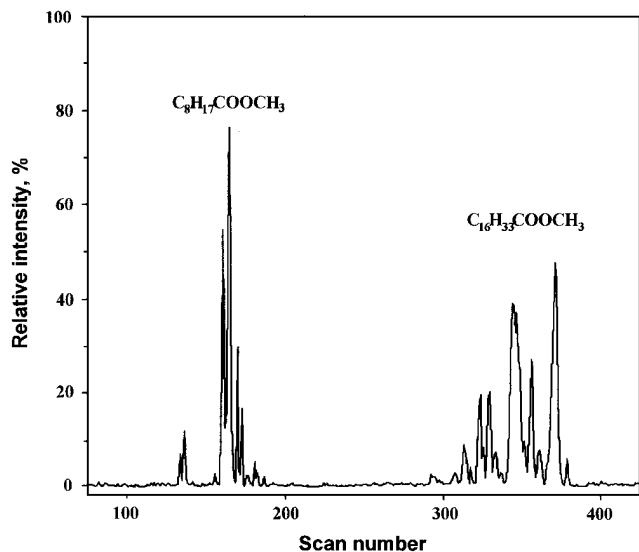


FIG. 8. GC-MS spectrogram of organic products extracted after dissolving the zeolite H-ZSM-5 in 10% NaOH solution. The zeolite sample contained octene-1, CO, and H<sub>2</sub>O coadsorbed in equal amount at 296 K. Before GC-MS analysis the expected carboxylic acids were converted in their methyl esters with CH<sub>2</sub>N<sub>2</sub>.

zeolite. The signals between 8 and 50 ppm may be attributed to aliphatic fragments of the acids, while those near 184–186 ppm may be attributed to COOH groups. The four most intense groups of signals in the aliphatic region at 14.7 ppm (quartets,  $J(\text{C,H}) = 125$  Hz), 23.4, 30.5 and 32.6 (all peaks around these signals are triplets,  $J(\text{C,H}) = 125$  Hz) can be attributed to the linear CH<sub>3</sub>CH<sub>2</sub>(CH<sub>2</sub>)<sub>*n*</sub> (*n* ≥ 1) fragments of the acids.

GC-MS analysis shows two main groups of organic products that are extracted from the zeolite and are considerably different in their retention time (Fig. 8). All peaks in both these two groups possess a characteristic value of  $m/e = 74$ , typical for methyl ester of fat carboxylic acids (55). Furthermore, some of the peaks in both groups exhibit in their mass spectra the signals from molecular ions characteristic for the methyl esters of the acids of the C<sub>8</sub>H<sub>17</sub>COOH family ( $m/e = 172$ ) and C<sub>16</sub>H<sub>33</sub>COOH family ( $m/e = 284$ ). Thus, on the basis of GC-MS analysis one can conclude that a mixture of at least nine C<sub>9</sub> and twelve C<sub>17</sub> carboxylic acids (see Fig. 8) is formed.

Note that contrary to ethene interaction with CO, where selective formation of the tertiary acid occurs, carbonylation of octene-1 on H-ZSM-5 results in the formation of a mixture of C<sub>9</sub> and C<sub>17</sub> carboxylic acids, with mainly linear CH<sub>3</sub>CH<sub>2</sub>(CH<sub>2</sub>)<sub>*n*</sub> (*n* ≥ 1) fragments prevailing in their structure. The reason for this may be that octene-1 molecule is already too large for the bulky tertiary carbenium cations to be easily generated from it and carbonylated in the narrow pores of H-ZSM-5.

It should be emphasized that these carboxylic acids are formed from octene-1 at room temperature. This fact

confirms that carbenium ions are indeed generated from octene-1 on H-ZSM-5 (19), and they can be chemically trapped with carbon monoxide. Preferential formation of the acids with linear hydrocarbon skeletons supports a suggestion made earlier on retaining the linear structure of octene-1 upon its adsorption inside H-ZSM-5 at room temperature (19).

#### 4. CONCLUSIONS

1. Using *in situ* <sup>13</sup>C solid state NMR (for some reagents in combination with *ex situ* GC-MS), butyl alcohols (*t*-BuOH, *i*-BuOH, and *n*-BuOH) and olefins (ethene, *iso*-butene, and octene-1) are shown to undergo carbonylation to form carboxylic acids (the Koch reaction) with high conversion on H-ZSM-5 zeolite at 296–373 K without application of pressurized conditions, just upon coadsorption of an alcohol and CO or an olefin, CO and H<sub>2</sub>O on the zeolite in stoichiometric amounts.

*t*-BuOH is carbonylated to form solely trimethylacetic acid with 100% conversion within a few days at 296 K and within 10 min at 373 K. *i*-BuOH is also converted solely into the same acid with 70% conversion within 1 h at 373 K. *n*-BuOH is slowly transformed at 373 K into 2-methylbutyric acid, in addition, much smaller amount of valeric acid and notable amounts of by-products (di-*n*-butyl ether and butene oligomers) are also formed.

In the presence of CO and H<sub>2</sub>O, *i*-C<sub>4</sub>H<sub>8</sub> at 296 K is carbonylated and hydrated with 100% conversion to form more than 80% trimethylacetic acid and less than 20% *t*-BuOH. Ethene reacts at 296 K with 40% conversion within a few hours to form mainly 2-methyl-2-ethylbutyric acid and a small amount of 1-methyl-1-ethylpropanol. Octene-1 produces a complicated mixture of the C<sub>8</sub>H<sub>17</sub>COOH and C<sub>16</sub>H<sub>33</sub>COOH acids with mainly linear hydrocarbon chains.

2. These reactions observed on zeolite H-ZSM-5 may open up new possibilities in using solid acids in organic synthesis as carbonylation catalysts under mild conditions, i.e., low temperature and normal atmospheric pressure.

3. Observation of Koch reaction under mild conditions strongly suggests the formation of alkyl carbenium ions on zeolites as crucial intermediate of the hydrocarbon conversion. Of the family of carbenium ions formed from butyl alcohols and olefins (isobutene, ethene, octene-1) in zeolite pores, CO reacts selectively with the tertiary cations to produce tertiary carboxylic acids unless narrow pores of H-ZSM-5 prevent the bulky tertiary cations to be generated from large carbonylated molecules (the case with octene-1).

#### ACKNOWLEDGMENTS

The research described in this publication was made possible in part by Grant No. RB 8000 from the International Science Foundation, in part by Grant No. RB 8300 from the International Science Foundation and

Russian Government, and by Grant No. 95-03-08780 from the Russian Foundation for Basic Research. One of the authors (A.G.S.) thanks Professor J. Sommer, Universite Louis Pasteur, Strasbourg, for the discussion on the chemistry of carbenium ions in superacids and on the possible ability to trap carbenium ions with CO in superacids (La Colle Sur Loup, Nice, France, 1993).

## REFERENCES

1. Germains, J. E., "Catalytic Conversion of Hydrocarbons." Academic Press, New York, 1969.
2. Jacobs, P. A., "Carbionogenic Activity of Zeolites," p. 86. Elsevier, Amsterdam, 1977.
3. Olah, G. A., *Angew. Chem.* **12**, 173 (1973).
4. Olah, G. A., Schilling, P., Staral, J. S., Halpern, Y., and Olah, J. A., *J. Am. Chem. Soc.* **97**, 6807 (1975).
5. Olah, G. A., Prakash, G. K. S., and Sommer, J., "Superacids." Wiley, New York, 1985.
6. Voge, H. H., in "Catalysis" (P. H. Emmett, Ed.), Vol. 6, p. 407. Reinhold, New York, 1958.
7. Liengme, B. V., and Hall, W. K., *Trans. Faraday Soc.* **62**, 3229 (1966).
8. Bolis, V., Vedrine, J. C., van den Berg, J. P., Wolthuizen, J. P., and Derouane, E. G., *J. Chem. Soc. Faraday Trans. 1* **76**, 1606 (1980).
9. Shigeishi, R., Garforth, A., Harris, I., and Dwyer, J., *J. Catal.* **130**, 423 (1991).
10. Kramer, G. M., McVicker, G. B., and Ziemiak, J. J., *J. Catal.* **92**, 355 (1985).
11. Lombardo, E. A., Dereppe, J. M., Marcelin, G., and Hall, W. E., *J. Catal.* **114**, 167 (1988).
12. Grady, M. C., and Gorte, R. J., *J. Phys. Chem.* **89**, 1305 (1985).
13. Aronson, M. T., Gorte, R. J., and Farneth, W. E., *J. Catal.* **105**, 455 (1987).
14. Aronson, M. T., Gorte, R. J., Farneth, W. E., and White, D., *J. Am. Chem. Soc.* **111**, 840 (1989).
15. Lazo, N. D., Richardson, B. R., Schettler, P. D., White, J. L., Munson, E. J., and Haw, J. F., *J. Phys. Chem.* **95**, 9420 (1991).
16. Stepanov, A. G., Romannikov, V. N., and Zamaraev, K. I., *Catal. Lett.* **13**, 395 (1992).
17. Stepanov, A. G., Zamaraev, K. I., and Thomas, J. M., *Catal. Lett.* **13**, 407 (1992).
18. Stepanov, A. G., and Zamaraev, K. I., *Catal. Lett.* **19**, 153 (1993).
19. Stepanov, A. G., Luzgin, M. V., Romannikov, V. N., and Zamaraev, K. I., *Catal. Lett.* **24**, 271 (1994).
20. Engelhardt, J., and Hall, W. K., *J. Catal.* **151**, 1 (1995).
21. Sommer, J., Hachoumy, M., Garin, F., and Barthomeuf, D., *J. Am. Chem. Soc.* **116**, 5491 (1994); Sommer, J., Hachoumy, M., Garin, F., Barthomeuf, D., and Vedrine, J., *J. Am. Chem. Soc.* **117**, 1135 (1995).
22. Stepanov, A. G., Sidelnikov, V. N., and Zamaraev, K. I., *Chem. Eur. J.* **2**, 157 (1996).
23. Haw, J. F., Richardson, B. R., Oshiro, I. S., Lazo, N. D., and Speed, J. A., *J. Am. Chem. Soc.* **111**, 2052 (1989).
24. Oliver, F. G., Munson, E. J., and Haw, J. F., *J. Phys. Chem.* **96**, 8106 (1992).
25. Kazansky, V. B., and Senchenya, I. N., *J. Catal.* **119**, 108 (1989); Kazansky, V. B., *Acc. Chem. Res.* **112**, 379 (1991).
26. Koch, H., *Brennstoff-Chemie* **36**, 321 (1955).
27. Bahrmann, H., in "New Syntheses with Carbon Monoxide" (J. Falbe, Ed.), p. 372. Springer-Verlag, Berlin, 1980.
28. Hogeveen, H., in "Advances in Physical Chemistry" (V. Gold, Ed.), Vol. 10, p. 29, 1973.
29. Stepanov, A. G., Luzgin, M. V., Romannikov, V. N., and Zamaraev, K. I., *J. Am. Chem. Soc.* **117**, 3615 (1995).
30. Romannikov, V. N., Mastikhin, V. M., Hočevár, S., and Držaj, V., *Zeolites* **3**, 311 (1983).
31. Harris, R. K., "Nuclear Magnetic Resonance Spectroscopy. A Physicochemical View," p. 107. Pitman, London, 1983.
32. Souma, Y., Sano, H., and Iyoda, J., *J. Org. Chem.* **38**, 2016 (1973).
33. Breitmaier, E., and Voelter, W., "<sup>13</sup>C NMR Spectroscopy, Methods and Applications in Organic Chemistry," p. 159. Verlag Chemie, Weinheim, 1978.
34. Anderson, M. W., and Klinowski, J., *J. Am. Chem. Soc.* **112**, 10 (1990); Munson, E. J., Lazo, N. D., Moellenhoff, M. E., and Haw, J. F., *J. Am. Chem. Soc.* **113**, 2783 (1991).
35. Bronnimann, C. E., and Maciel, G. E., *J. Am. Chem. Soc.* **108**, 7154 (1986).
36. (a) Engelhardt, G., and Michel, D., "High Resolution Solid State NMR of Silicates and Zeolites," p. 420. Wiley, Chichester, 1987. (b) Takasugi, M., Watanabe, N., and Niki, E., *Busei Kagaku* **30**, 504 (1981).
37. Fyfe, C. A., "Solid State NMR for Chemists," Chaps. 5 and 6. CFC Press, Guelph, 1983.
38. Delavarenne, S., Simon, M., Fauconet, M., and Sommer, J., *J. Chem. Soc. Chem. Commun.*, 1049 (1989); Delavarenne, S., Simon, M., Fauconet, M., and Sommer, J., *J. Am. Chem. Soc.* **111**, 383 (1989); Bukala, J., Culmann, J.-C., and Sommer, J., *J. Chem. Soc. Chem. Commun.*, 4581 (1992); Sommer, J., and Bukala, J., *Acc. Chem. Res.* **26**, 370 (1993).
39. Williams, C., Makarova, M. A., Malysheva, L. V., Paukshtis, E. A., Talsi, E. P., Thomas, J. M., and Zamaraev, K. I., *J. Catal.* **127**, 377 (1991).
40. Hoelderich, W., Reuvers, J., Kummer, R., and Hupfer, L., Eur. Patent, 249976, December 23, 1987.
41. Williams, C., Makarova, M. A., Malysheva, L. V., Paukshtis, E. A., Zamaraev, K. I., and Thomas, J. M., *J. Chem. Soc. Faraday Trans.* **86**, 3473 (1990).
42. Marr, D. H., *Org. Magn. Res.* **13**, 28 (1980).
43. Makarova, M. A., Paukshtis, E. A., Thomas, J. M., Williams, C., and Zamaraev, K. I., *J. Catal.* **149**, 36 (1994).
44. Stepanov, A. G., Luzgin, M. V., Paukshtis, E. A., and Zamaraev, K. I., in preparation.
45. Terentev, A. B., and Dostovalova, V. I., *Org. Magn. Res.* **9**, 301 (1977).
46. Couperus, P. A., Clague, H. P., and Dongen, J. P. C., *Org. Magn. Res.* **11**, 590 (1978).
47. Van den Berg, J. P., Wolthuizen, J. P., Clague, A. D. H., Hays, G. R., Huis, R., and van Hooff, J. H. C., *J. Catal.* **80**, 130 (1983).
48. Munson, E. J., Kheir, A. A., Lazo, N. D., and Haw, J. F., *J. Phys. Chem.* **96**, 7740 (1992).
49. Datema, K. P., Novak, A. K., van Braam Houkgeest, J., and Wielers, A. F. H., *Catal. Lett.* **11**, 267 (1991).
50. Olah, G. A., Parker, D. G., and Yoneda, N., *J. Am. Chem. Soc.* **98**, 2245 (1976).
51. Williamson, K. L., Clutter, D. R., and Emch, R., *J. Am. Chem. Soc.* **96**, 1471 (1974).
52. Kokotailo, G. T., Lowton, S. L., Olson, D. H., and Meier, W. M., *Nature (London)* **272**, 437 (1978).
53. Souma, Y., and Sano, H., *Bull. Chem. Soc. Jpn.* **47**, 1717 (1974).
54. Breitmaier, E., and Voelter, W., "<sup>13</sup>C NMR Spectroscopy, Methods and Applications in Organic Chemistry," p. 173. Verlag Chemie, Weinheim, 1978.
55. Budzikiewicz, H., Djerassi, C. D., and Williams, D. H., "Interpretation of Mass Spectra of Organic Compounds." Holden-Day, Inc., San Francisco, 1964.